The American Journal of Pathology, Vol. 171, No. 3, September 2007

DOI: 10.2353/ajpath.2007.060991

Epithelial and Mesenchymal Cell Biology

Targeted Skin Overexpression of the Mineralocorticoid Receptor in Mice Causes Epidermal Atrophy, Premature Skin Barrier Formation, Eye Abnormalities, and Alopecia

Yannis Sainte Marie,* Antoine Toulon,* Ralf Paus,† Eve Maubec,‡ Aicha Cherfa,* Maggy Grossin,§ Vincent Descamps,‡ Maud Clemessy,¶ Jean-Marie Gasc,¶ Michel Peuchmaur,‖ Adam Glick,** Nicolette Farman,* and Frederic Jaisser*

From INSERM U772, Collège de France, Université Paris-Descartes, Paris, France; the Department of Dermatology,† University Hospital Schleswig-Holstein, University of Luebeck, Luebeck, Germany; the Service de Dermatologie,‡ Hôpital Bichat, Paris, France; the Service d'Anatomopathologie,§ Hôpital Louis Mourier, Colombes, France; INSERM U833,¶ Collège de France, Paris, France; the Equipe EA 3102,‖ Service d'Anatomopathologie, Hôpital Robert Debré, Paris, France; and Center for Molecular Toxicology and Carcinogenesis,** Pennsylvania State University, University Park, Pennsylvania*

The mineralocorticoid receptor (MR) is a transcription factor of the nuclear receptor family, activation of which by aldosterone enhances salt reabsorption in the kidney. The MR is also expressed in nonclassical aldosterone target cells (brain, heart, and skin), in which its functions are incompletely understood. To explore the functional importance of MR in mammalian skin, we have generated a conditional doxycycline-inducible model of MR overexpression, resulting in double-transgenic (DT) mice [keratin 5-tTa/tetO-human MR (hMR)], targeting the human MR specifically to keratinocytes of the epidermis and hair follicle (HF). Expression of hMR throughout gestation resulted in early postnatal death that could be prevented by antagonizing MR signaling. DT mice exhibited premature epidermal barrier formation at embryonic day 16.5, reduced HF density and epidermal atrophy, increased keratinocyte apoptosis at embryonic day 18.5, and premature eye opening. When hMR expression was initiated after birth to overcome mortality, DT mice developed progressive alopecia and HF cysts, starting 4 months after hMR induction, preceded by dystrophy and cycling abnormalities of pelage HF. In contrast, interfollicular epidermis, vibrissae, and footpad sweat glands in DT mice were normal. This new mouse model reveals novel biological roles of MR signaling and offers an instructive tool for dissecting nonclassical functions of MR signaling in epidermal, hair follicle, and ocular physiology. ***(Am J Pathol 2007, 171:846–860; DOI: 10.2353/ajpath.2007.060991)***

The skin forms an epithelial barrier that protects the body from environmental damage. This barrier is generated by the epidermis and its constituent cells, most of which are keratinocytes, organized into constantly renewing layers. The basal layer of epidermal keratinocytes is highly proliferative and gives rise to suprabasal layers committed to terminal differentiation that migrate to the surface to produce the stratum corneum, the external cornified layer.[1] The epidermis also gives rise to skin appendages, such as hair follicles, the epithelial component of which is principally formed by keratinocytes and the development (and growth) of which is a highly controlled dynamic process.[2,3]

Epidermal and hair follicle keratinocytes are highly susceptible to regulation by nuclear receptors.[4–9] Nuclear receptors are transcription factors that regulate various cell functions throughout the body. The nuclear receptor superfamily includes the glucocorticoid receptor (GR), the mineralocorticoid receptor (MR), sex steroid and thyroid hormone receptors, vitamin D and retinoic acid receptors, peroxisome proliferator-activated recep-

Supported by INSERM, by the Centre de Recherche Industrielle et Technique, and a Ph.D. grant from NUCLEIS and Agence Nationale de Valorisation de la Recherche (to Y.S.M.).

Accepted for publication June 19, 2007.

Supplemental material for this article can be found on *http://ajp.amjpathol.org*.

Address reprint requests to Nicolette Farman, INSERM U772, Collège de France, 11 Place Marcelin Berthelot, 75005 Paris, France. E-mail: nicolette.farman@college-de-france.fr.

tors, and numerous orphan receptors.[10] In the skin, members of this family prominently participate in the control of epidermal and hair follicle development, differentiation, and remodeling, and key ligands of nuclear receptors are potent modulators of keratinocyte growth.[4–9] For example, thyroid hormone stimulates epidermal proliferation and hair growth,[11] whereas vitamin D derivatives, retinoids, and glucocorticoids inhibit keratinocyte proliferation, which is exploited for treating chronic hyperproliferative skin diseases like psoriasis.[12] The potency of glucocorticoids as inhibitors of keratinocyte proliferation is mirrored by their cutaneous side effects (eg, epidermal and dermal atrophy, resulting in thin and fragile skin).[13]

The MR is crucial for body fluid homeostasis. On binding the mineralocorticoid hormone aldosterone, the renal MR activates transcription of several genes that ultimately upregulate renal sodium reabsorption, thus contributing to regulation of extracellular fluid volume and blood pressure.[14] At variance with its closest homolog, the ubiquitous GR, the MR is expressed in a more limited number of target cells. In addition to the classical mineralocorticoid-sensitive epithelial tissues (the distal parts of the renal tubule, the colonic epithelium, and the excretory ducts of sweat and salivary glands), the MR is also expressed in some nonepithelial cells (neurons and cardiomyocytes) in which its functions are not fully understood.[14] Interestingly, the MR was also found (mRNA and protein) in human epidermis and hair follicles.[15] High levels of MR transcripts were also reported in murine skin,[16] where—due to absence of sweat glands—MR is unlikely to play a major role in fluid homeostasis. Some clinical observations point to the possibility that the aldosterone-MR system may be involved in epidermal and/or hair growth abnormalities. An association was noted between baldness and coronary diseases and/or hypertension, classical outcomes of states of hyperaldosteronism.[17,18] The MR antagonist spironolactone is frequently used to treat hirsutism and occasionally androgenetic alopecia, which has been classically attributed to the antagonism of androgen receptors by spironolactone and its interference with steroidogenesis.[4,19,20] Mammalian skin also displays classical downstream effectors of the aldosterone-MR signaling cascade. The epithelial sodium channel ENaC involved in aldosterone-dependent sodium reabsorption[14,21] is also expressed in human and rat epidermal keratinocytes and hair follicle[22,23]; genetic disruption of the ENaC α-subunit in mice leads to epidermal hyperplasia and abnormal epidermal terminal differentiation.[24] Moreover, genetic disruption of the ENaC-activating serine-protease CAP1 also leads to severe impairment of skin barrier permeability.[25] However, the actual functions of MR in skin physiology and pathology are still completely obscure.

To investigate the role of the MR in the skin, we have generated a conditional transgenic model to control MR expression[26] selectively in keratinocytes (and not in other aldosterone target cells) by use of the keratin 5 (K5) promoter.[27] Because transgene expression is inducible, it permits either embryonic or postnatal expression of the MR. Whereas embryonic MR expression led to early postnatal death preceded by epidermal atrophy and apoptosis, postnatal MR expression resulted in progressive alopecia and formation of hair follicle cysts without alterations of interfollicular epidermis and keratinocyte-derived appendages.

Materials and Methods

This study conforms to the standards of INSERM (the French National Institute of Health) regarding the care and use of laboratory animals and was performed in accordance with European Union Council Directives (86/609/EEC).

Generation of the Human MR Conditional Model

Skin conditional expression of human MR (hMR) in double-transgenic (DT) mice was obtained by crossing the previously characterized tetO-hMR mice L2 line[26] with the K5-tTA transactivator mouse strain derived from founder 1216, kindly provided by Dr. A. Glick.[27] Both strains were crossed on B6D2 genetic background. Genotypes were determined by polymerase chain reaction (PCR) co-amplification of hMR (forward, 5′-AACTAAgTgTCCCAACAATT-3′, and reverse, 5′-gAAAAgAAAATAAgAggAgACAATgg-3′) or tTA (forward, 5′-AACAACCCgTAAACTCgCCCAgAAg-3′, and reverse, 5′-CgCAACCTAAAgTAAAATgCCCCAC-3′) and actin (forward, 5′-gTgTTAgACACTgTggACATgg-3′, and reverse, 5′-gAgAgAgCCATACCAAgAATgg-3′) from tail genomic DNA using recombinant *Taq* (Invitrogen, Cergy-Pontoise, France) in conditions described by the supplier. Heterozygous tetO-hMR and K5-tTA were crossed to produce DT mice and study genotype distribution at different ages. In some experimental series, the hMR strain was bred to homozygosity and used to produce DT mice. Monotransgenic tetO-hMR, K5-tTA, and wild-type mice did not differ in skin phenotype, indicating that the observed phenotype of DT (K5-tTA/tetO-hMR) mice was not due to the position of transgene insertion into the genome or to tTA transactivator expression. Monotransgenic mice were therefore used as controls of their DT littermates.

Reverse Transcription-PCR Analysis

Dorsal skin tissues or organs were frozen in liquid nitrogen. Total RNA was isolated by mechanical disruption in TRIzol (Invitrogen) directly for embryos' skin or after grinding under liquid nitrogen in a mortar (Biospec, Bartesville, OK) for adult skin. RNAs from organs were further purified using cationic resin column from RNeasy kit (Qiagen, Courtaboeuf, France). First-strand cDNA were synthesized after DNase I treatment (DNAfree; Ambion, Huntingdon, UK) using 1 μg of total RNA, random hexamers (Amersham, Saclay, France), and Superscript II reverse transcriptase (Invitrogen). Transgene expression was analyzed as previously described[26] using β2-microglobulin or 18S as internal controls (β2-microglobulin: forward, 5′-TTCTATATC-CTGGCTCACACTGAA-3′, and reverse, 5′-CACAT-GTCTCGATCCCAGTAGA-3′; and 18S: forward, 5′-C-CCTGCCCTTTGTACACACC-3′, and reverse, 5′-CGA-

TCCGAGGGCCTCATCA-3′). Transcripts levels of mouse MR, human MR, ENaC subunits, Gpx3, Dusp10, and glyceraldehyde-3-phosphate dehydrogenase expression were analyzed by real-time PCR performed in a iCycler iQ apparatus (Bio-Rad Laboratories LifeSciences, Marnes La Coquette, France) with SYBR Green I detection. PCR was performed in triplicate for each sample using a qPCR Core kit for SYBR Green I (Eurogentec, Seraing, Belgium) containing 300 nmol/L of specific primers and 3 μl of diluted template cDNA in a 25-μl total volume. Serial dilutions of pooled cDNA were used in each experiment to assess PCR efficiency. Expression of hMR relative to mouse MR (mMR) was estimated on the same run and with the same fluorescence threshold by Δcycle threshold calculation after assessment that PCR efficiency was 100%; results were adjusted to amplicon length.

The following primers were used. mMR: forward, 5′-TCACATTTTTAACATGTGACGGC-3′, and reverse, 5′-CTTAGTCAGCTCAGGCTTGCC-3′; hMR: forward, 5′-TGCTTCTACACCTTCCGAGAGTC-3′, and reverse, 5′-ACACCAGCCACCACCTTCTGATAG-3′; αENaC: forward, 5′-CGGAGTTGCTAAACTCAACATC-3′, and reverse, 5′-TGGAGACCAGTACCGGCT-3′; βENaC: forward, 5′-ATGTGGTTCCTGCTTACGCTG-3′, and reverse, 5′-GTCCTGGTGGTGTTGCTGTG-3′; γENaC: forward, 5′-CCAAAGCCAGCAAATAAACAAA-3′, and reverse, 5′-GCGGCGGGCAATAATAGAGA-3′; Gpx3: forward, 5′-AAACAGGAGCCAGGCGAGAACT-3′, and reverse, 5′-CCCgTTCACATCTCCTTTCTCAAA-3′; and Dusp10: forward, 5′-AGCCACAGACAGCAACAAAC-3′, and reverse, 5′-CATCAAGTAGGCGATGACGA-3′. The reference gene was glyceraldehyde-3-phosphate dehydrogenase: forward, 5′-AATGGTGAAGGTCGGTGTG-3′, and reverse, 5′-GAAGATGGTGATGGGCTTCC-3′.

Pharmacological Treatments

Mice were fed standard chow (A04; Scientific Animal Food Engineering, Epinay sur Orge, France) and drank tap water ad libitum. When required, food containing 1g/kg doxycycline (DOX; Sigma-Aldrich, La Verpilliere, France) was provided to mothers from mating until weaning of their offsprings. The MR antagonist potassium canrenoate (Sigma-Aldrich) was provided in the drinking water during pregnancy to yield 40 mg kg^{-1} day^{-1}.

Morphology

Skin biopsies matched for age and body sites or embryos (head and dorsal skin) were fixed in 4% phosphate-buffered paraformaldehyde and embedded in paraffin. Five-micrometer sections were stained with hematoxylin and eosin.

Immunohistochemistry and Immunofluorescence

Parafin-embedded sections were deparaffinized in xylene, hydrated in a graded alcohol series, and washed in phosphate-buffered saline (PBS). Ki 67 histochemistry and terminal deoxynucleotide transferase dUTP nick-end labeling (TUNEL) assay were performed as previously described.[28] In brief, Ki 67 histochemistry was done after antigen retrieval by heating in citrate buffer and inactivation of endogenous peroxidase by 1% H_2O_2 treatment. Slides were successively incubated with blocking agent (1/10; Power Block; Biogenex, San Ramon, CA), with rabbit anti-Ki 67 antibody (1/400; Novacastra, Newcastle on Tyne, UK), with goat anti-rabbit antibody (1/100; Santa Cruz, Heidelberg, Germany) and finally with peroxidase-conjugated rabbit anti-goat antibody (1/100; Dako, Trappes, France). Ki 67 antigen was revealed with 3,3′-diaminobenzidine tetrahydrochloride (Dako), and sections were counterstained with hematoxylin. For TUNEL assay, slides were treated with 0.05% pepsin (Sigma-Aldrich); elongation of the DNA fragments was achieved using digoxigenin coupled-11-dUTP (Enzo, Farmingdale, NY) and 0.5 U of TdT (Amersham) for 60 minutes at 37°C in a humid incubator. The reaction was stopped and after washing in 10 mmol/L Tris-HCl, digoxigenin was detected with alkaline phosphatase-conjugated anti-digoxigenin antibodies (1/200; Enzo). Cleaved caspase 3 was detected using a polyclonal antibody (1/100; Cell Signaling, Ozyme, Saint Quentin en Yvelines, France) that was revealed using an avidin-biotin kit.

Immunohistochemistry of the MR was performed on paraformaldehyde-fixed skin sections from mice 1 month after DOX withdrawal (allowing hMR expression in DT mice) and in embryonic day (E) 18.5 DT embryos. Two monoclonal antibodies[29] (kindly provided by C. Gomez-Sanchez, Division of Endocrinology, University of Mississippi Medical Center, Jackson, MS) were used: 2D6 (1/100), which was raised against a peptide that differs by three amino acids between mouse and human MR and labels essentially the endogenous mMR (not hMR), and 6G1 antibody (1/100), which was raised against a peptide entirely homologous between mouse and human MRs, and labels the endogenous MR and the transgenic hMR. Paraffin-embedded sections were deparaffinized and hydrated, and the nonspecific signal was reduced by the use of the MOM kit (Mouse On Mouse; Vector, AbCys, Paris, France) according to the manufacturer's recommendations. Sections were incubated for 30 minutes with MR-specific antibodies and rinsed in PBS, followed by a streptavidin-based detection system. Amplification of the signal was obtained with the TSA kit (Tyramide Signal Amplification; Perkin Elmer, Courtaboeuf, France) according to the manufacturer's recommendations. The mouse IgG UPC10 (1/5000; Sigma-Aldrich) was used as a nonimmune control.

Immunofluorescence was performed on 10-μm cryostat sections of unfixed frozen skin samples. Sections were postfixed for 20 minutes at room temperature with methanol (10 minutes) and permeabilized with 0.25% Nonidet P-40. Primary antibodies (incubated overnight at 4°C) were as follows: anti-K1 (1/500), anti-K10 (1/100), anti-loricrine (1/250), anti-filaggrin (1/2000), kindly provided by E. Hummler (Institut de Pharmacologie, Univer-

sité de Lausanne, Lausanne, Switzerland),[25] anti-ZO1 (1/100; Zymed; Invitrogen), and anti-occludin (1/100; Zymed); secondary antibody was Cy3-goat anti-rabbit (1/200; Jackson ImmunoResearch Laboratories, West Grove, PA). Nuclei were labeled with Sytox green (Molecular Probes, Eugene, OR) for 5 minutes in the dark. Fluorescence was examined under confocal microscope (Zeiss Meta LSM 510; Mannheim, Germany).

Western Blot

The expression of the mouse glucocorticoid receptor mGR was measured on skin from E18.5 embryos by Western blot, using the M20 anti-GR antibody (1/1000; Santa Cruz) as described by the supplier.

Collection of Embryos

K5-tTA and tetO-hMR mice were mated during the night, and presence of vaginal plug next morning was considered as gestational day 0.5. Embryos were collected by cesarean section at 14.5, 16.5, or 18.5 gestational days around 11:00 AM. Newborn pups from three litters were collected just after birth.

Skin Permeability Assay

E16.5 embryos were processed as described previously[30] for toluidine blue staining assay. In brief, embryos were successively immersed under shaking in 100% methanol for 1 minute in PBS and then in 0.1% toluidine blue in PBS for 3 minutes and rinsed several times in PBS until excess blue was removed. Treated embryos were photographed by digital camera (Nikon, Melville, NY), and the tail was cut off for genotyping. The different patterns of skin barrier permeability described for control mice between embryonic days 16 and 17[30] were used to score (1 to 8) and to compare semiquantitatively barrier formation status in DT and control embryos.

Depilation Experiments

In this series, DOX treatment was provided throughout gestation and interrupted at birth. Pups were wax-depilated at postnatal day 21 as described previously[31]; skin samples were collected either at day 6 or at day 14 after depilation for histological examination (hematoxylin and eosin staining).

Morphometry

The NIH Image J software (Bethesda, MD) was used to measure epidermis thickness and hair follicle density per millimeter of epidermis in E18.5 skin sections.

Statistical Analysis

Data are provided as mean values and SEM. Comparison between control and DT mice was done using Student's *t*-test. Genotype distributions were compared for each condition (age and treatment) using χ^2 test to expected Mendelian distribution considering theoretical size as 25% of total number of mice. Barrier permeability score distributions were analyzed using χ^2 test (results were grouped into two classes, scores 1 to 4 and scores 5 to 8, and compared).

Results

In the Absence of Doxycycline, Double-Transgenic Mice Overexpress the hMR in the Skin

The DT mice (K5-tTa/tetO-hMR) express the hMR in keratin 5-expressing epithelia, including the basal layer of

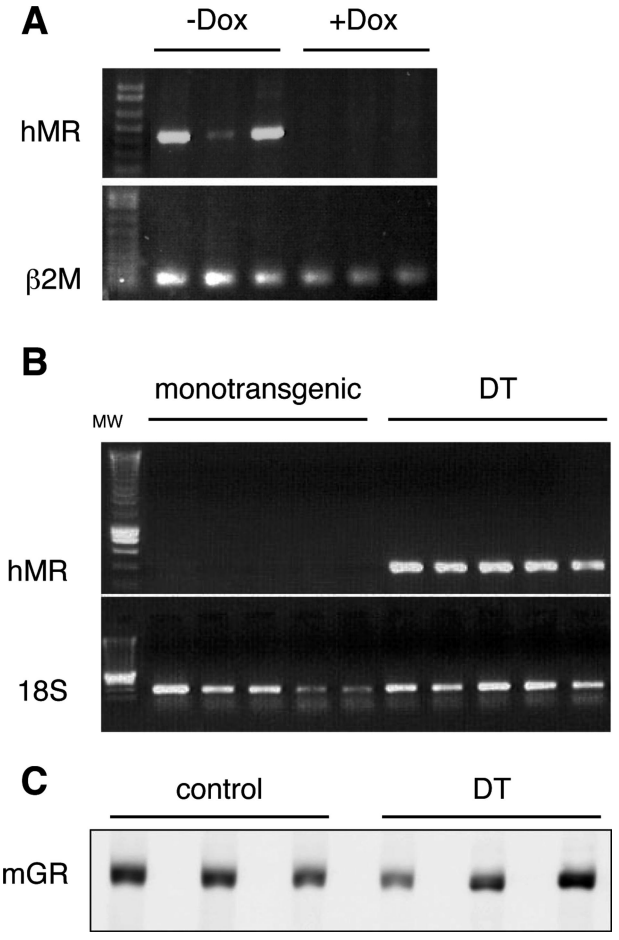

Figure 1. Conditional hMR expression in the skin. **A:** hMR mRNA expression [as determined by reverse transcription (RT)-PCR] in dorsal skin of adult double-transgenic DT (K5-tTA/tetO-hMR) mice: hMR is expressed in the absence of DOX, whereas 15-day DOX administration (provided in the food) fully suppressed hMR expression. β2-Microglobulin was used as internal standard (different mice in each lane). **B:** hMR expression (RT-PCR) in the skin of five monotransgenic (control) embryos and five DT embryos (E18.5). The transgene was detected only in DT mice. 18S signal was used as internal standard. **C:** Western blot of the mouse GR in the skin of three control and three DT embryos (E18.5). Quantification of signal (normalized to Ponceau staining) showed similar GR expression in control mice (arbitrary units: 1.17 ± 0.07) and hMR-overexpressing DT mice (1.08 ± 0.11), $n = 5$ embryos in each group.

epidermal keratinocytes and the outer root sheath of the hair follicle.[27] As shown in Figure 1A, administration of DOX to double-transgenic mice results in complete extinction of transgene expression in DT skin. In the absence of DOX, the expression of hMR is detectable only in DT mice (Figure 1B).

A real-time PCR comparison of endogenous mMR and exogenous hMR mRNA levels showed an apparent

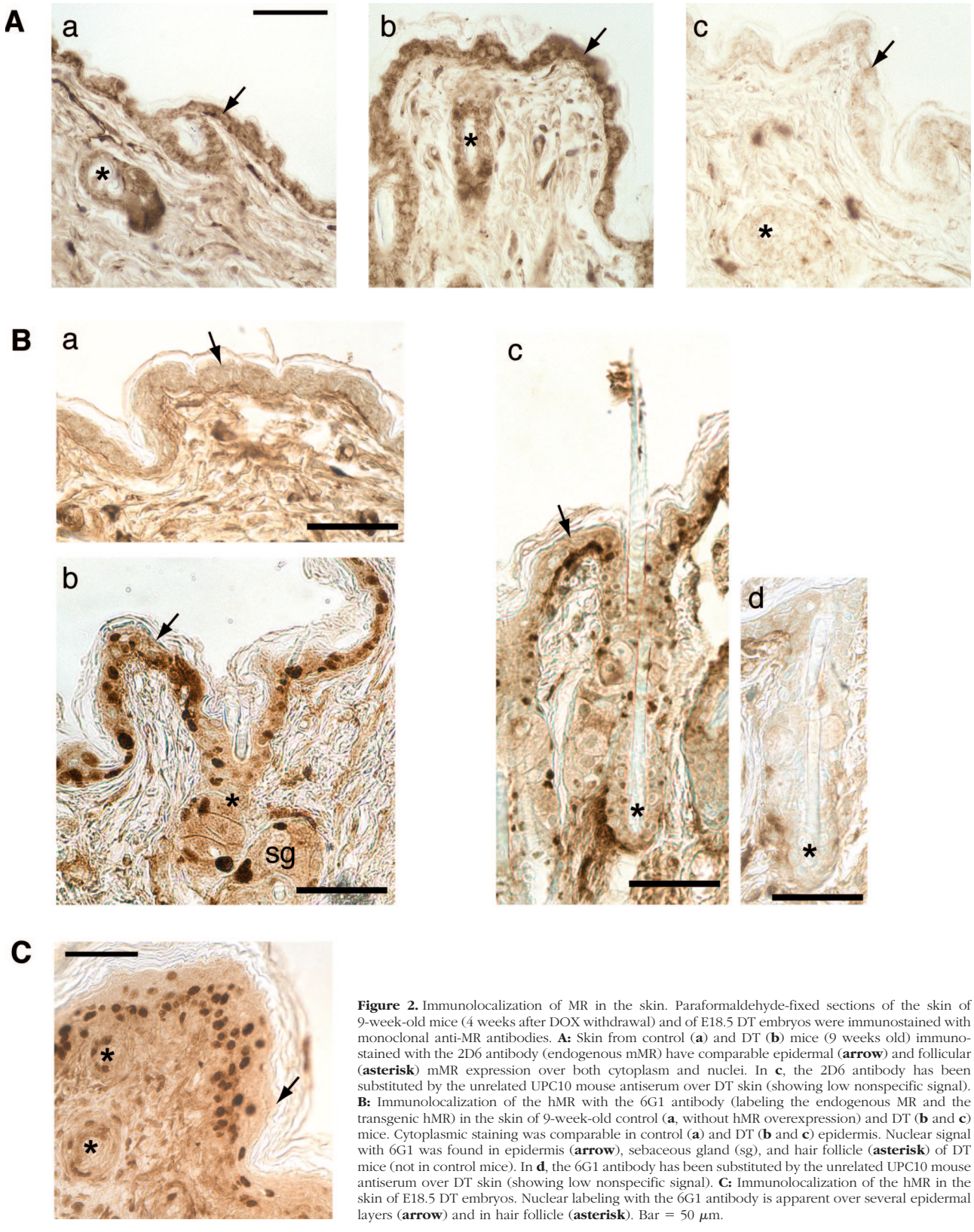

Figure 2. Immunolocalization of MR in the skin. Paraformaldehyde-fixed sections of the skin of 9-week-old mice (4 weeks after DOX withdrawal) and of E18.5 DT embryos were immunostained with monoclonal anti-MR antibodies. **A:** Skin from control (**a**) and DT (**b**) mice (9 weeks old) immunostained with the 2D6 antibody (endogenous mMR) have comparable epidermal (**arrow**) and follicular (**asterisk**) mMR expression over both cytoplasm and nuclei. In **c**, the 2D6 antibody has been substituted by the unrelated UPC10 mouse antiserum over DT skin (showing low nonspecific signal). **B:** Immunolocalization of the hMR with the 6G1 antibody (labeling the endogenous MR and the transgenic hMR) in the skin of 9-week-old control (**a**, without hMR overexpression) and DT (**b** and **c**) mice. Cytoplasmic staining was comparable in control (**a**) and DT (**b** and **c**) epidermis. Nuclear signal with 6G1 was found in epidermis (**arrow**), sebaceous gland (sg), and hair follicle (**asterisk**) of DT mice (not in control mice). In **d**, the 6G1 antibody has been substituted by the unrelated UPC10 mouse antiserum over DT skin (showing low nonspecific signal). **C:** Immunolocalization of the hMR in the skin of E18.5 DT embryos. Nuclear labeling with the 6G1 antibody is apparent over several epidermal layers (**arrow**) and in hair follicle (**asterisk**). Bar = 50 μm.

ratio of hMR over mMR of 6.97 ± 1.00 in E18.5 DT mice ($n = 4$) and of 1.72 ± 0.40 in adult DT mice ($n = 3$); this ratio is only an estimate because the efficiency of reverse transcription may differ between mMR and hMR mRNA.

MR Overexpression Does Not Alter Intracutaneous GR Expression and Is Unlikely to Cause Cofactor Deprivation for GR and Vitamin D Receptor

Figure 1C shows that mGR levels (immunoblot analysis) were similar between the skin of E18.5 control and hMR-overexpressing DT mice. Thus, MR overexpression is not associated with obvious changes in GR protein levels.

No significant differences were found in the expression (real-time PCR) of a glucocorticoid-sensitive gene (Gpx3[32]) and of a vitamin D-regulated gene (Dusp10[33]) between control embryos (Gpx3, 0.34 ± 0.06, $n = 4$ embryos; Dusp10, 1.38 ± 0.26, $n = 5$) and DT embryos (Gpx3, 0.42 ± 0.07, $n = 6$; Dusp10, 1.18 ± 0.19, $n = 6$). Thus, MR overexpression does not seem to impair GR and vitamin D receptor activity (at least with respect to the two sensitive marker genes tested).

Keratinocytes express the sodium channel ENaC,[22–24] a classical aldosterone-MR target.[21] In the skin of E18.5 hMR-expressing embryos, we did not find any significant difference between DT littermates ($n = 6$) and their control littermates ($n = 5$) in the expression levels of ENaC α-, β-, or γ-subunit transcripts, as measured by real-time PCR (not shown). Hence, it is unlikely that abnormal ENaC expression could play a role in the observed skin phenotype of DT mice.

MR Expression in Situ *Is Prominent in Murine Epidermal and Hair Follicle Keratinocyte*

The MR was demarcated at the protein level, using two different monoclonal antibodies generated by C. Gomez Sanchez.[29] Figure 2, A and B, illustrates MR immunolocalization experiments performed in 9-week-old mice; in this series, DOX treatment was stopped 5 weeks after birth, thus allowing hMR expression for 4 weeks in DT mice. The mouse MR (2D6 antibody) was found in the epidermis and hair follicle, without substantial differences in immunoreactivity between control and DT mice (Figure 2A, a and b). As previously reported,[29] the 2D6 antibody detected both cytoplasmic and nuclear mMR. Cytoplasmic staining was also observed in the epidermis of control and DT mice with the 6G1 antibody (Figure 2B, a–c). The hMR was detectable using the 6G1 antibody over all layers of the epidermis and in the hair follicle and sebaceous gland epithelium (Figure 2B, b and c) only in the DT mice, with variable but clear nuclear localization. Such differential, antibody-dependent localization of MR immunostaining has been documented previously,[29] likely due to conformational states of the receptor, either bound to chaperone proteins or in its activated nuclear state.[29] It must be noted that the intensity of immunostaining is dependent on antibody affinities for the exposed epitope and does not correlate with absolute levels of mMR versus hMR. The specificity of the staining observed with 2D6 or 6G1 is assessed by the low level of signal (Figure 2, Ac and Bd) yielded when these antibodies are substituted by an unrelated monoclonal antibody (UPC10). Figure 2C shows hMR immunoreactivity (using the 6G1 antibody) in the skin of E18.5 DT embryos: the signal is seen in the same epithelial compartments as in adult DT mice and is not substantially higher than that observed in adults (Figure 2B), despite the differences in hMR-to-mMR mRNA ratios between these two age groups. Interestingly, the hMR was found not only in the K5-specific basal layer of the epidermis but also in upper differentiating layers of the epidermis, indicating that it is a relatively long-lived protein.

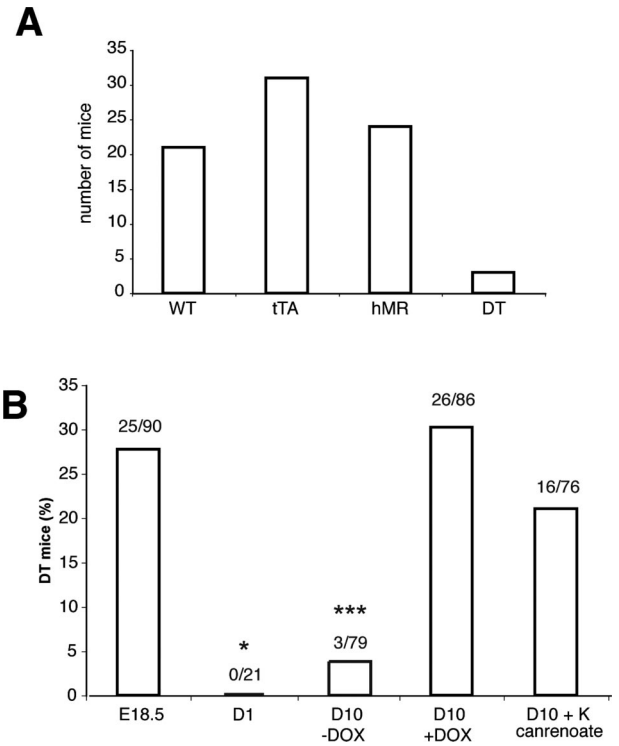

Figure 3. Conditional hMR expression in the skin during gestation provokes perinatal mortality. **A:** Number of mice alive at postnatal day 10 according to their genotype: wild-type (WT), monotransgenic tTA or hMR (K5-tTA or tetO-hMR), and DT (K5-tTA/tetO-hMR) pups. A major deficiency of DT mice was observed at day 10, attesting for their earlier mortality. **B:** DT mice recovered at E18.5 (ie, 1 day before birth), at postnatal day 1 (D1), and at day 10 (D10); results are expressed as the percentage of DT mice among offspring. At E18.5, the number of DT mice was close to that expected, ie, 25% (according to Mendelian distribution), whereas DT mice were all dead at the end of day 1, indicating perinatal mortality of DT mice. Administration of DOX or the MR antagonist potassium canrenoate during gestation prevented the mortality of DT pups, as seen in surviving treated DT pups at day 10. Numbers above bars indicate the number of DT versus total mice in each series. $^{*}P < 0.05$; $^{***}P < 0.001$; χ^2 test.

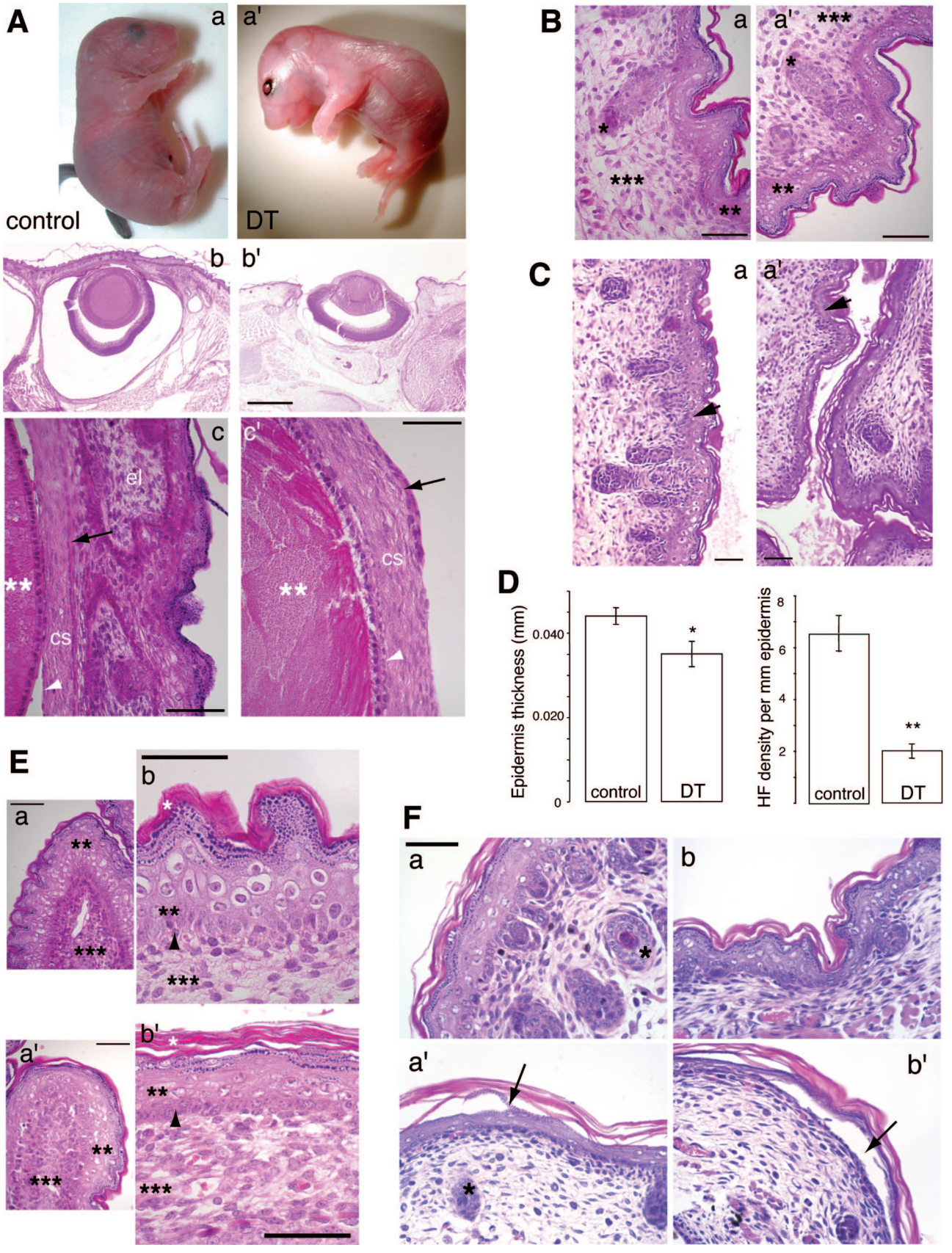
A
a
a'
control
DT
b
b'
c
c'
el
cs
B
a
a'
C
a
a'
D
Epidermis thickness (mm)
0.040
0.020
0
control
DT
HF density per mm epidermis
8
6
4
2
control
DT
E
a
b
a'
b'
F
a
b
a'
b'

Expression of hMR in Mouse Epidermis during Embryogenesis Causes Early Postnatal Mortality, Which Is Preventable by MR Antagonist Administration

Initial experiments showed that in the absence of doxycycline, most mice found after birth were monotransgenic mice (K5-tTA or tetO-hMR) or wild-type mice: only three DT mice were present at day 10 out of 79 pups (Figure 3A). However, when DOX was provided to the mother at the beginning of the pregnancy to suppress hMR expression, double-transgenic mice were born at the expected frequency (Figure 3B). Fetuses were collected at days E14.5 and E18.5 and at the end of day 1 (it is important to note here that birth occurs within 8 to 24 hours after E18.5 in our mouse strains). Although no DT pups were found in this series at the end of day 1 (0 out of 21 pups), the expected amount of DT embryos were present at E14.5 (not shown) and E18.5 (Figure 3B). In addition, pups from another series collected within 5 to 10 minutes after birth were all alive, controls and DT mice (representing 22% of 23 pups). Importantly, mortality of the double-transgenic mice could also be prevented by treating the pregnant mice with potassium canrenoate, the major spironolactone metabolite, to antagonize the MR (Figure 3B), indicating the MR dependency of lethality. Thus overexpression of hMR causes rapid death of the DT mice after birth.

The DT embryos collected at E18.5 had similar body weight compared with their control littermates yet presented with abnormally smooth, shiny, dry, erythematous skin (Figure 4A, a′). Survival of these E18.5 DT mice was comparable with that of their control littermates (4 to 5 hours) when placed in a 37°C thermostated chamber (not shown), indicating that they do not exhibit major life-threatening malformation.

hMR Overexpression in Murine Skin Epithelium during Embryogenesis Causes Ocular Abnormalities

The eyes of all control embryos were closed at E18.5 (Figure 4A, a), whereas DT littermates presented with an eye-open phenotype (21 of 25 DT embryos) (Figure 4A, a′). In DT E18.5 embryos, prominent developmental defects of the anterior eye were noted (Figure 4A, b′ and c′): The eyelids were absent, and DT mice had dysplasic corneal epithelium with zones of complete aplasia of this epithelium (Figure 4A, c′), whereas the corneal stroma appeared normal. The corneal endothelium exhibited extensive adhesion to the lens in DT mice, resulting in obliteration of the anterior eye chamber (Figure 4A, c′). As expected, there was no alteration of the retina in DT mice (the K5 promoter is inactive there).

K5-Driven hMR Overexpression during Embryogenesis Causes a Severe Skin Phenotype, Characterized by Epidermal Atrophy

Histology of skin of E18.5 DT and control mice from the same integumental sites showed significant reduction in epidermal thickness and flat epidermis in the skull (Figure 4B), ear (Figure 4E), and abdominal skin (Figure 4C) in DT mice. Figure 4D shows a quantification of this difference for abdominal skin. High-magnification photographs illustrate the marked reduction of the granular layer of the epidermis (Figure 4E; compare b from control and b′ from DT mice), but there were no consistent differences in the stratum corneum between control and DT E18.5 mice. E18.5 DT mice also exhibited reduced density of hair follicles (Figure 4D).

Examination of the skin of DT mice at the time of birth showed a dramatic accentuation of the epidermal phenotype (Figure 4F, compare a and b from controls and a′ and b′ from DT mice), with epidermal atrophy, zones of intraepidermal separation (Figure 4F, a′ and b′, arrow), and a general tendency of the stratum corneum to detach from the epidermal granular layer of the epidermis. In contrast, the tooth germs, the palate, and the nasal septum were unaltered in DT mice (Supplemental Figure S1 at *http://ajp.amjpathol.org*).

hMR Overexpression Does Not Alter Epidermal Keratinocyte Proliferation but Causes Excessive Keratinocyte Apoptosis in E18.5 Embryos

The Ki 67 staining in the basal layer of the epidermis was comparable in control and DT mice (Figure 5A). In the E18.5 DT skin, TUNEL-positive cells were distributed throughout all epidermal layers and were sometimes grouped in clusters of apoptotic cells (Figure 5A), whereas in control mice, only rare TUNEL-positive kera-

Figure 4. Phenotype of MR-expressing embryos. Expression of hMR during development impairs skin and eye formation at E18.5 and leads to skin atrophy at birth. **A:** E18.5 DT embryos (**a′**) presented with a shiny erythematous skin and open eyes compared with their control littermates (**a**). Low-magnification view of the eye (bar = 250 μm) of E18.5 control (**b**) and DT (**b′**) embryos (hematoxylin-eosin staining): At this stage of development the eyelids are fully formed and fused in control embryos, whereas in DT mice, they are poorly developed and do not cover the eye, leading to the eye-open phenotype (also note the thin epidermis in DT mice). High-magnification view (bar = 50 μm) of the anterior eye of control (**c**) and DT (**c′**) embryos: eyelids (el) cover the cornea of controls only (in **c**); the corneal epithelium (**arrow**) is partly absent in DT (**c′**) embryos; the anterior chamber [between the corneal stroma (cs) and the lens (**)] is obliterated in DT embryos. **White arrowhead**, corneal endothelium. **B:** Skin of the skull of control (**a**) and DT (**a′**) E18.5 embryos. The morphology of hair follicle (**asterisk**) is comparable in control and DT embryos. Bar = 50 μm; **, epidermis; ***, dermis. **C:** Abdominal skin of control (**a**) and DT (**a′**) E18.5 embryos illustrating the flat and thinner epidermis and the reduction in the density of hair follicles (HF) in DT mice; **arrow**, epidermis; bar = 40 μm. **D:** Quantification of the epidermis thickness in abdominal skin of control and E18.5 DT embryos (n = 5 controls and 6 DT embryos; average number of measurements, 268 per embryo) and hair follicle (HF) density per millimeter of epidermis (n = 5 controls and 5 DT embryos; 528 HF counted in controls, 220 in DT mice). *$P < 0.05$; **$P < 0.001$. **E:** Skin covering the ear in control (**a** and **b**) and DT (**a′** and **b′**) E18.5 embryos at low (**a** and **a′**) and high (**b** and **b′**) magnification. *, stratum corneum; **, epidermis; ***, dermis; **arrowhead**, basal layer of keratinocytes. Note the epidermal hypoplasia with the reduction of the granular layer (just below the stratum corneum) in DT mice. Bar = 50 μm. **F:** Skin of control (**a** and **b**) and DT (**a′** and **b′**) mice at birth (5 to 10 minutes after birth). Abdominal (**a** and **a′**) and dorsal (**b** and **b′**) skin is atrophic in DT mice, with intraepidermal zones of rupture (**arrow**) and loosely adhering stratum corneum (**a′** and **b′**). The **arrow** denotes a split right above basal layer of keratinocytes in DT epidermis. Bar = 50 μm.

tinocytes were found in the uppermost, differentiated layers of the epidermis. Labeling with an anti-cleaved caspase 3 antibody showed only a few positive cells in each genotype; however, caspase-3-positive cells were clearly visible only in the most superficial epidermal layer of DT mice (not shown). These results, together with the histological evidence of epidermal atrophy, suggest that hMR overexpression in murine epidermis causes keratinocyte apoptosis, or premature cell death normally associated with terminal differentiation.[34]

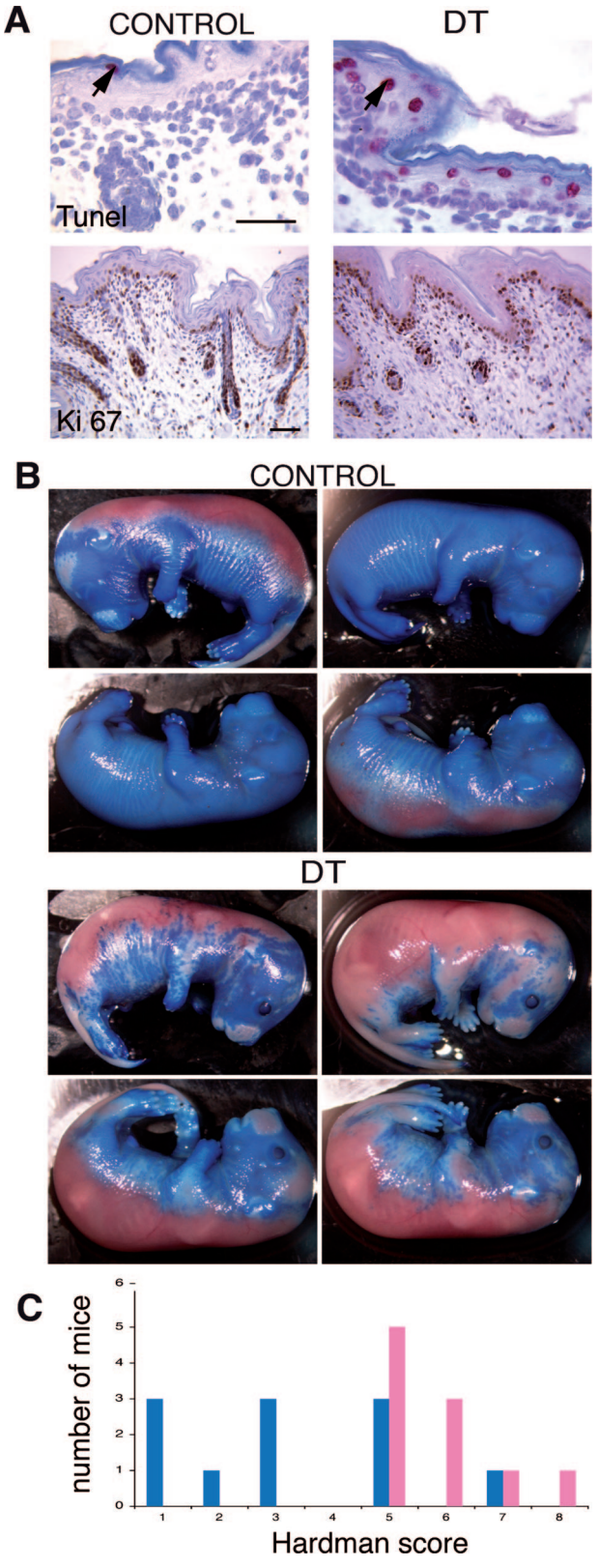

hMR Overexpression Induces Premature Epidermal Barrier Formation at E16.5

In the mouse, formation of an impermeable skin barrier occurs between E16 and E17, following a precise spatiotemporal pattern.[30] To determine whether overexpression of hMR caused changes in the skin barrier, we examined the permeability of fetal epidermis to toluidine blue. At E16.5, the majority of control embryos did not have a fully efficient epidermal barrier, with the greatest impermeability localized to the back and hindquarter skin. In contrast, at the same gestational age, the epidermis of DT embryos was much less toluidine blue-permeable, and the region of impermeability was more widespread (Figure 5B), leading to a much higher impermeability score in DT embryos than in their control littermates (Figure 5C). Thus hMR overexpression induces premature dye impermeability of the epidermal barrier at E16.5.

Despite this evidence suggesting premature skin barrier formation at E16.5 in DTs, 2 days later (E 18.5), there was no obvious change in the immunoreactivity for several key markers of keratinocyte differentiation (cytokeratin K1 and K10, loricrine and filaggrin, or the tight junctions proteins ZO1 and occludin) (data not shown).

Postnatal Overexpression of hMR in Keratinocytes Results in a Striking Hair Phenotype, Characterized by Alopecia, Abnormal Hair Follicle Cycling, Hair Follicle Dystrophy, and Cystic Degeneration

In E18.5 DT embryos, there was a threefold reduction in hair follicle density (Figure 4D), whereas there was no apparent change in vibrissae. To characterize further this hair phenotype, hMR overexpression was induced by DOX removal after weaning. At about 5 months of age, DT mice developed progressive hair loss that began in

Figure 5. Expression of hMR during development leads to increased apoptosis at E18.5 and accelerated skin barrier formation at E16.5. **A:** Proliferation and apoptosis in the skin of E18.5 embryos. TUNEL assay showed an increased number of apoptotic cells (TUNEL-positive red nuclei, **arrow**) in the epidermis of DT mice compared with their control littermates (bar = 50 μm). Ki 67 staining showed no difference in cell proliferation between controls and DT mice (bar = 40 mm). **B:** Toluidine blue test of epidermal permeability in E16.5 embryos (Hardman test). Most control embryos had a highly permeable skin (extensive blue staining), whereas DT embryos have large portions of the skin that are impermeable to toluidine blue (pink aspect), indicating that expression of hMR during development accelerates skin barrier formation at E16.5. **C:** Hardman scoring (see Materials and Methods) of the degree of epidermal impermeability, from completely permeable blue skin (score 1) to completely impermeable pink skin (score 8). E16.5 DT embryos (pink bars) have higher impermeability score than controls (blue bars). $P < 0.01$, χ^2 test.

the dorsal neck region and in ventral skin and subsequently extended to large stretches of dorsal skin. By 8 to 9 months, the DT mice expressing hMR had a generalized hairless phenotype or sparse, patchy fur coat (Figure 6A). In contrast to pelage hair follicles, whiskers were fully preserved in DT mice.

To establish the histopathology and kinetics of hair phenotype development, repetitive skin biopsies were performed in a series of 33 mice from the age of 5 weeks (when DOX was withdrawn) to the age of 6 months (midventral region) (Table 1). Two weeks after DOX withdrawal (Figure 6C), control ($n = 18$) and DT ($n = 15$) mice had a comparable hair coat and largely indistinguishable hair follicles that were mostly located deep in the dermis/subcutis, indicating that the majority of these follicles was in the anagen (growth) stage of the hair cycle. In the anagen stage, hair follicles reach down into the subcutis and show an inner root sheath rich in trichohyalin granules and a pigmented hair shaft, whereas regressing or resting hair follicles (catagen, telogen) reside in the dermis.[31] One month after induction of MR (Figure 6D), control mice displayed mostly very short hair follicles without inner root sheaths, whereas two-thirds of DT mice showed hair follicles that remained deep in the subcutis. This suggests that MR overexpression causes an abnormality of hair follicle cycling (ie, delayed catagen entry). This conclusion is supported by additional histological evidence that clearly shows that the majority of DT mice display anagen hair follicles, whereas control skin shows telogen follicles (Supplemental Figure S2 at *http://ajp.amjpathol.org*).

To obtain more insight into the hair cycling abnormalities of DT mice, wax-depilation experiments were performed in 3-week-old mice, ie, in mice that had spontaneously entered their first resting stage of the hair cycle (telogen), and anagen was induced by depilation (in this series, DOX was stopped just after birth).[35] As expected, 6 days after depilation, the skin of control mice was pigmented (indicating advanced anagen development), whereas DT mice were still pink (indicating that most of the depilated hair follicles were still in telogen or early anagen). Fourteen days after depilation, there were islands of fur coat, surrounded by alopecic (nude) skin in DT mice, whereas all control mice showed prominent hair growth. Skin histomorphometry at day 14 after depilation showed that the dermis thickness, which is strictly hair cycle-dependent,[31] differed significantly between control and DT mice ($19 \pm 2\%$ total skin thickness in control mice ($n = 5$), and $26 \pm 2\%$ total skin thickness in DT mice ($n = 5$), $P < 0.05$). These data demonstrate a greatly retarded depilation-induced anagen development in the skin of DT mice.

Further iterative biopsies of skin revealed a slowly progressive appearance of hair follicle abnormalities in DT mice, leading eventually to cystic hair follicle degeneration. Nine weeks after DOX withdrawal, the majority of DT mice showed signs of hair follicle dystrophy (ectopic melanin granules, melanin incontinence, and malformed inner and outer root sheaths; Figure 6E). This was hardly ever seen in control mice. No inflammatory cells were seen in DT mice. After 12 weeks, this became even more prominent, accompanied by a relative asynchrony of hair follicle cycling, as indicated by the simultaneous presence of telogen and anagen hair follicles next to each other (Figure 6F). Such asynchrony was never seen in control mice. After 22 weeks, cystic degeneration of the hair follicle was prominent in DT skin (Figure 6, G and H; Table 1) yet never seen in control mice.

Table 1 summarizes the kinetics of the observed abnormalities and quantifies the number of dermal cysts in DT mice. The lag time required to yield alopecia and histological cysts in DT mice was relatively long (about 16 weeks after the induction of MR expression). In contrast to hair follicles, no changes were observed in the histological aspect or thickness of the interfollicular epidermis of DT mice. Whisker follicles (vibrissae), footpad sweat glands, and esophageal mucosa (a pluristratified epithelium) were also normal in DT mice. Thus, postnatal MR overexpression affects selectively pelage hair follicles, without altering the structure of the interfollicular epidermis or other keratinocyte-derived appendages.

The Hair Phenotype of hMR-Overexpressing Mice Is Associated with Abnormalities in Hair Follicle Proliferation and Apoptosis

Epidermal Ki 67 staining was similar between the adult mice of both genotypes; in contrast, there was an increase in Ki 67 staining in the inner and outer root sheath of the hair follicle of the adult DT mice expressing hMR compared with follicles from control mice (Figure 6B). In addition, there were some apoptotic cells in hair follicles of DT mice, as monitored by TUNEL and immunohistochemical detection of cleaved caspase 3, but these were extremely rare in the control mice (not shown). Thus the formation of hair follicle cysts in DT mice is accompanied by hyperproliferation and some degree of apoptosis in follicular keratinocytes in the absence of patent inflammation.

Discussion

Genetic manipulation of several nuclear hormone receptors has revealed important roles in epidermal and hair follicle biology. Constitutive overexpression of the glucocorticoid receptor[36–38] in the basal layer of the epidermis produces a phenotype that resembles human ectodermal dysplasia.[39] K5-GR embryos have epidermal alterations ranging from smooth and thin skin with epidermal hypoplasia and underdeveloped dysplastic hair follicles and vibrissae to complete disruption of the cutaneous barrier and absence of skin at the cranial and umbilical regions.[38] In addition, these mice have an open-eye phenotype, proptosis of the ocular globe, and epithelial defects of the cornea,[37] and defects in tooth and palate development were also noted.[36] GR-null mice, which die immediately after birth because of their inability to reabsorb the fluid filling the lungs, have reduced keratinization of the epidermis at birth, indicating impaired maturation of the skin.[40] Genetic disruption of the retinoic X receptor-α in epidermal keratinocytes and

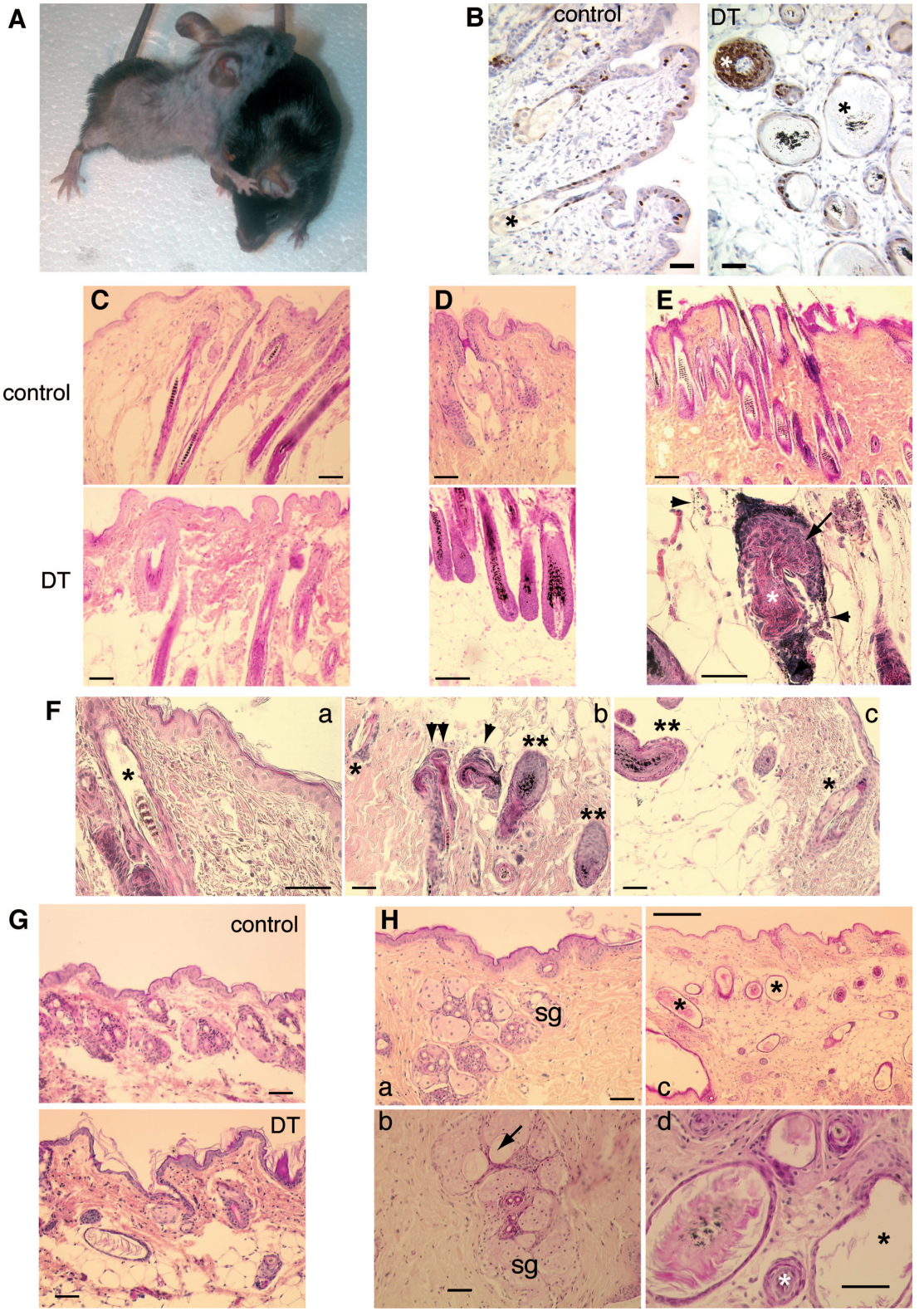
A
B
control
DT
C
D
E
control
DT
F
a
b
c
G
control
DT
H
sg
a
c
b
sg
d

Table 1. Kinetics of Appearance of Skin Abnormalities

Weeks after DOX withdrawal	Dermal cysts per field (*n*)	Abnormalities in DT	Figure
2	0	None: HF in dermis (anagen) in control and DT; normal fur	Figure 6C
4	0	Delayed entry into catagen/telogen; normal fur	Figure 6D; Supplemental Figure 2
9	0	Signs of HF dystrophy in DT; no HF dystrophy seen in controls	Figure 6E
12	1.35 ± 0.39 (Nine DT mice)*	Histological appearance of few dermal cysts; macroscopic fur appearance still normal	Figure 6F
16	2.00 ± 0.31 (Six DT mice)*	Onset of macroscopically visible alopecia (moderate); dermal cysts	Figure 6G
22	3.95 ± 0.48 (Eight DT mice)*	Irregular diffuse hair loss; progressive cystic degeneration of HF and sebaceous glands	Figure 6H
25	4.26 ± 0.42 (Seven DT mice)*	Further progression of alopecia; numerous dermal cysts	

Mice received DOX during development and early postnatal life, up to the age of 5 weeks; DOX was then withdrawn to allow hMR expression, and iterative biopsies were performed. ORS, outer root sheath.
*No cysts seen in control mice.

hair follicle results in destruction of hair follicle architecture, formation of epidermal utriculi, dermal cysts, and progressive alopecia.[41] Vitamin D receptor knockout also leads to progressive hair loss,[42,43] showing that these receptors play a key role in hair cycle and terminal differentiation of interfollicular epidermis. However, these two nuclear receptors seem to be dispensable for embryonic development. This current study using a conditional expression model reveals that overexpression of the MR, a nuclear receptor closely related to GR, causes severe alterations in both the neonatal and adult mouse.

Prenatal MR overexpression causes an eye-open phenotype[44,45] (that could be due to a defect in eyelid development or to eyelid apoptosis), reduced hair follicle formation, premature formation of the permeability barrier at E16.5, and an atrophic epidermis with evidence of an abnormally high degree of keratinocyte apoptosis at E18.5. Reduced thickness of the epidermis was particularly evident in the granular layer. Although the premature epidermal barrier formation in DT skin at E16.5 strongly suggests enhanced terminal differentiation, this does not provide definitive evidence for accelerated epidermal differentiation (there may have been a dissociation of skin lipid formation and keratinocyte differentiation; this possibility is underscored by the subsequent absence of changes in the immunoreactivity for key markers of epidermal differentiation). The role of MR-mediated signaling in keratinocyte differentiation remains to be further dissected.

In addition, these mice die shortly after birth. Despite the premature barrier formation seen in E16.5 DT mice, the atrophic epidermis may fail to execute full protective functions at birth, with diminished capacity to adapt to the skin shear-stress associated with delivery, leading to excessive water and heat loss and subsequent death. In addition, the skin atrophy may also cause maternal negligence. These hypotheses warrant further testing.

The phenotype observed in MR-overexpressing embryos is less severe than that induced by GR overexpression, and it is limited to the epidermis, hair follicle, and cornea, without prenatal alterations in vibrissae, teeth, or palate. Thus MR-overexpressing mice do not display typical features of ectodermal dysplasia. It is also interesting to note that no obvious skin defect has been reported in MR knockout mice, which die 10 days after birth from severe renal salt loss,[46] indicating that the MR is dispensable for prenatal skin development.

Postnatal MR overexpression produces delayed (at least 4 months) alopecia and dermal cysts, which are preceded by hair follicle dystrophy and abnormalities of hair follicle cycling, without alteration of the interfollicular epidermis. The alopecia and dermal cyst formation is not a scratching-induced artifact because we have not ob-

Figure 6. Cutaneous phenotype of adult control and DT mice. Postnatal expression of hMR results in alopecia and hair follicle cysts. Mice were fed with DOX food from the onset of gestation until the age of 5 weeks, and then DOX was withdrawn to allow MR expression. **A:** An adult 8-month-old DT mouse (**left**) with extensive alopecia compared with its control littermate (**right**). **B:** Ki 67 staining of the skin of adult (6 months) control and DT mice, showing the increased proliferation in the multilayered hair follicle cysts (**white asterisk**) in DT mice. **Asterisk** indicates HF in control and dilated hair follicle cysts in DT mice. Bar = 50 μm. **C–H:** Consecutive biopsies of murine skin at different time intervals after DOX withdrawal (on week 5 after birth), illustrating the progressive appearance of hair follicle abnormalities and cystic hair follicle degeneration. Lag time after DOX withdrawal: **C**, 2 weeks; **D**, 4 weeks; **E**, 9 weeks; **F**, 12 weeks; **G**, 16 weeks; and **H**, 22 weeks. Bars: 200 μm (in **H**, **c**); 50 μm (in all other panels). **C:** Two weeks after DOX withdrawal, no abnormalities are visible in DT skin. **D:** Four weeks after DOX withdrawal, control mice show telogen hair follicles, whereas DT skin shows mature anagen hair follicles, as indicated by their characteristic morphology, location (deep in subcutis), and pigmentation (Supplemental Fig. S2 for further evidence of anagen, available at *http://ajp.amjpathol.org*), suggesting an abnormality in hair follicle cycling. **E:** Nine weeks after DOX withdrawal, many microscopic fields of DT skin exhibited signs of severe hair follicle dystrophy [as evident from the presence of ectopic melanin granules, melanin incontinence (**arrowheads**), and malformed inner (**white asterisk**) and outer (**arrow**) root sheaths]. This was seen only very rarely and, when present, in a more discrete manner in control skin of this age group. **F:** Twelve weeks after DOX withdrawal, the skin of DT mice continued to show signs of hair follicle dystrophy, as evidenced by dilated hair canal (**asterisk** in **a**) and abnormal hair follicle (HF) architecture and pigmentation (**b**) as well as of relative asynchrony of hair follicle cycling, as indicated by the simultaneous presence of telogen and anagen hair follicles next to each other (**b** and **c**; *, telogen HF; **, anagen HF; **arrowhead**, dystrophic anagen HF; **double arrowhead**, dystrophic telogen/catagen HF). **G:** Sixteen weeks after DOX withdrawal, dermal cysts of HF were apparent in several DT mice, not in controls. **H:** Histology of the skin 22 weeks after DOX withdrawal in control [**a**, sebaceous glands (sg)] and DT (**b–d**) mice. Cysts of sebaceous glands (**b**, **arrow**) and of hair follicle (*, **c** and **d**) in DT mice are shown. See Table 1 for comments.

served any differences in grooming or scratching behavior between control and DT mice and because older DT mice present with a generalized, irregular "moth-eaten" alopecia that is not consistent with localized scratching or grooming (Figure 6A). The pathogenesis of the hair phenotype described here, mechanistically, cannot yet be explained. However, cystic hair follicle degeneration is a standard response pattern of irreversibly damaged hair follicles leading to alopecia.[47]

In mouse skin,[16] retinoic X receptor, retinoic acid receptor, GR, and MR are among the most prominently represented nuclear receptors at the mRNA level. It is likely that the phenotype of our DT mice is directly related to targets of MR overexpression and not because of indirect effects through squelching activities of other nuclear receptors via reduction in availability of coactivators/repressors[48] because we observed no significant changes in mRNA expression of two target genes for the GR and vitamin D receptor in MR-overexpressing mice.

In contrast to the mineralocorticoid-sensitive cells of the kidney, the epidermis does not express the MR-protector enzyme 11 β-hydroxysteroid dehydrogenase type 2 that prevents illicit renal MR occupancy by glucocorticoid hormones.[14,15] Thus, in the skin, the MR should be predominantly occupied by glucocorticoid hormones, which largely prevail in the plasma and which can bind to MR as well as GR, rather than by aldosterone. It is interesting to note that the skin atrophy observed in MR-overexpressing embryos is reminiscent of the epidermal abnormalities resulting from glucocorticoid administration. Exposure of skin to glucocorticoids[49–51] accelerates the maturation of the epidermal permeability barrier in rat embryos; in humans, treatment with glucocorticoids (general or topical) induces atrophy of the epidermis and dermis, causing a major concern to patients.[13]

Recent research has opened a fascinating new view of skin endocrinology, because the integument and its appendages not only are highly sensitive to many hormones but also can produce them,[7,52–54] thus forming a local stress response system analogous to the hypothalamus-pituitary-adrenal axis.[52,55] The skin is a steroidogenically active organ[52,53]: skin cells (particularly within hair follicle) can produce corticosteroids, including DOC, 18OH-DOC, corticosterone, and cortisol (human) but not aldosterone, in a process that is cell-type specific.[56–60] Importantly, because aldosterone synthesis does not occur, this should favor the onset of glucocorticoid-occupied MR complexes. Local cortisol synthesis within the hair follicle[52] can transactivate the GR and the MR, and this new endocrine unit could participate in skin homeostasis and possibly skin pathologies. In the light of the current findings, it is tempting to hypothesize that a disturbed balance of corticosteroid receptor activation (altered expression or occupancy) in the skin produces excessive occupancy of the MR by glucocorticoids in keratinocytes, leading to skin alterations such as those found in this study. The association of MR antagonists to dermocorticoids should therefore be considered to limit the undesirable side effects of glucocorticoids.

It has been reported that immunosuppressive drugs, such as cyclosporin A, inhibit the transcriptional activity of the MR.[61] It is worth noting that treatment of transplanted patients with cyclosporin A is often accompanied by hirsutism[62]; cyclosporin A also induces hair growth in mice,[63] ie, a mirror image of the results yielded in our mouse model, in which MR overexpression produces alopecia. Thus increased MR activity may be inversely linked to hair growth. Therefore MR antagonism (specific for the MR and devoid of androgen receptor affinity) may be beneficial in subjects prone to alopecia or baldness.

In conclusion, this conditional transgenic approach of MR overexpression in keratinocytes has revealed two distinct phenotypes, one occurring during embryonic development and leading to early postnatal death and another developing after birth. These results should allow identification of novel MR signaling pathways in nontraditional aldosterone target cells and potential MR-dependent therapeutic strategies for human skin diseases.

Acknowledgments

We thank Francoise Cluzeaud for immunofluorescence experiments, Raphael Rambur for his help in the iconography, and Olivier Thibaudeau for expert histology techniques. We thank Dr. Celso Gomez-Sanchez for his kind gift of anti-MR antibodies. We are indebted to Francine Behar-Cohen for her help in eye analysis and to Ariane Berdal for careful examination of tooth and palate.

References

1. Blanpain C, Fuchs E: Epidermal stem cells of the skin. Annu Rev Cell Dev Biol 2006, 22:339–373
2. Schmidt-Ullrich R, Paus R: Molecular principles of hair follicle induction and morphogenesis. Bioessays 2005, 27:247–261
3. Stenn KS, Paus R: Controls of hair follicle cycling. Physiol Rev 2001, 81:449–494
4. Alonso LC, Rosenfield RL: Molecular genetic and endocrine mechanisms of hair growth. Horm Res 2003, 60:1–13
5. Calléja C, Messaddeq N, Chapellier B, Yang H, Krezel W, Li M, Metzger D, Mascrez B, Ohta K, Kagechika H, Endo Y, Mark M, Ghyselinck NB, Chambon P: Genetic and pharmacological evidence that a retinoic acid cannot be the RXR-activating ligand in mouse epidermis keratinocytes. Genes Dev 2006, 20:1525–1538
6. Icre G, Wahli W, Michalik L: Functions of the peroxisome proliferator-activated receptor (PPAR) α and β in skin homeostasis, epithelial repair, and morphogenesis. J Investig Dermatol Symp Proc 2006, 11:30–35
7. Ohnemus U, Uenalan M, Inzunza J, Gustafsson JA, Paus R: The hair follicle as an estrogen target and source. Endocr Rev 2006, 27:677–706
8. Bikle DD, Elalieh H, Chang S, Xie Z, Sundberg JP: Development and progression of alopecia in the vitamin D receptor null mouse. J Cell Physiol 2006, 207:340–353
9. Radoja N, Stojadinovic O, Waseem A, Tomic-Canic M, Milisavljevic V, Teebor S, Blumenberg M: Thyroid hormones and gamma interferon specifically increase K15 keratin gene transcription. Mol Cell Biol 2004, 24:3168–3179
10. Lu NZ, Wardell SE, Burnstein KL, Defranco D, Fuller PJ, Giguere V, Hochberg RB, McKay L, Renoir JM, Weigel NL, Wilson EM, McDonnell DP, Cidlowski JA: International Union of Pharmacology. LXV. The pharmacology and classification of the nuclear receptor superfamily: glucocorticoid, mineralocorticoid, progesterone, and androgen receptors. Pharmacol Rev 2006, 58:782–797
11. Safer JD, Crawford TM, Holick MF: Topical thyroid hormone accelerates wound healing in mice. Endocrinology 2005, 146:4425–4430
12. Pèrez A, Chen TC, Turner A, Raab R, Bhawan J, Poche P, Holick MF: Efficacy and safety of topical calcitriol (1,25-dihydroxyvitamin d3) for the treatment of psoriasis. Br J Dermatol 1996, 134:238–246

13. Schäcke H, Docke WD, Asadullah K: Mechanisms involved in the side effects of glucocorticoids. Pharmacol Ther 2002, 96:23–43
14. Farman N, Rafestin-Oblin ME: Multiple aspects of mineralocorticoid selectivity. Am J Physiol 2001, 280:F181–F192
15. Kenouch S, Lombes M, Delahaye F, Eugene E, Bonvalet JP, Farman N: Human skin as target for aldosterone: coexpression of mineralocorticoid receptors and 11 β-hydroxysteroid dehydrogenase. J Clin Endocrinol Metab 1994, 79:1334–1341
16. Bookout AL, Jeong Y, Downes M, Yu RT, Evans RM, Mangelsdorf DJ: Anatomical profiling of nuclear receptor expression reveals a hierarchical transcriptional network. Cell 2006, 126:789–799
17. Lotufo PA, Chae CU, Ajani UA, Hennekens CH, Manson JE: Male pattern baldness and coronary heart disease: the Physicians' Health Study. Arch Intern Med 2000, 160:165–171
18. Matilainen VA, Makinen PK, Keinanen-Kiukaanniemi SM: Early onset of androgenetic alopecia associated with early severe coronary heart disease: a population-based, case-control study. J Cardiovasc Risk 2001, 8:147–151
19. Moghetti P, Tosi F, Tosti A, Negri C, Misciali C, Perrone F, Caputo M, Muggeo M, Castello R: Comparison of spironolactone, flutamide, and finasteride efficacy in the treatment of hirsutism: a randomized, double blind, placebo-controlled trial. J Clin Endocrinol Metab 2000, 85:89–94
20. Sinclair R: Chronic telogen effluvium: a study of 5 patients over 7 years. J Am Acad Dermatol 2005, 52:12–16
21. Rossier BC, Pradervand S, Schild L, Hummler E: Epithelial sodium channel and the control of sodium balance: interaction between genetic and environmental factors. Annu Rev Physiol 2002, 64:877–897
22. Brouard M, Casado M, Djelidi S, Barrandon Y, Farman N: Epithelial sodium channel in human epidermal keratinocytes: expression of its subunits and relation to sodium transport and differentiation. J Cell Sci 1999, 112:3343–3352
23. Roudier-Pujol C, Rochat A, Escoubet B, Eugene E, Barrandon Y, Bonvalet JP, Farman N: Differential expression of epithelial sodium channel subunit mRNAs in rat skin. J Cell Sci 1996, 109:379–385
24. Mauro T, Guitard M, Behne M, Oda Y, Crumrine D, Komuves L, Rassner U, Elias PM, Hummler E: The ENaC channel is required for normal epidermal differentiation. J Invest Dermatol 2002, 118:589–594
25. Leyvraz C, Charles RP, Rubera I, Guitard M, Rotman S, Breiden B, Sandhoff K, Hummler E: The epidermal barrier function is dependent on the serine protease CAP1/Prss8. J Cell Biol 2005, 170:487–496
26. Ouvrard-Pascaud A, Sainte-Marie Y, Benitah JP, Perrier R, Soukaseum C, Cat AN, Royer A, Le Quang K, Charpentier F, Demolombe S, Mechta-Grigoriou F, Beggah AT, Maison-Blanche P, Oblin ME, Delcayre C, Fishman GI, Farman N, Escoubet B, Jaisser F: Conditional mineralocorticoid receptor expression in the heart leads to life-threatening arrhythmias. Circulation 2005, 111:3025–3033
27. Diamond I, Owolabi T, Marco M, Lam C, Glick A: Conditional gene expression in the epidermis of transgenic mice using the tetracycline-regulated transactivators tTA and rTA linked to the keratin 5 promoter. J Invest Dermatol 2000, 115:788–794
28. Saadi-Kheddouci S, Berrebi D, Romagnolo B, Cluzeaud F, Peuchmaur M, Kahn A, Vandewalle A, Perret C: Early development of polycystic kidney disease in transgenic mice expressing an activated mutant of the β-catenin gene. Oncogene 2001, 20:5972–5981
29. Gomez-Sanchez CE, de Rodriguez AF, Romero DG, Estess J, Warden MP, Gomez-Sanchez MT, Gomez-Sanchez EP: Development of a panel of monoclonal antibodies against the mineralocorticoid receptor. Endocrinology 2006, 147:1343–1348
30. Hardman MJ, Sisi P, Banbury DN, Byrne C: Patterned acquisition of skin barrier function during development. Development 1998, 125:1541–1552
31. Müller-Röver S, Handjiski B, van der Veen C, Eichmuller S, Foitzik K, McKay IA, Stenn KS, Paus R: A comprehensive guide for the accurate classification of murine hair follicles in distinct hair cycle stages. J Invest Dermatol 2001, 117:3–15
32. Tuckermann JP, Reichardt HM, Arribas R, Richter KH, Schutz G, Angel P: The DNA binding-independent function of the glucocorticoid receptor mediates repression of AP-1-dependent genes in skin. J Cell Biol 1999, 147:1365–1370
33. Lu J, Goldstein KM, Chen P, Huang S, Gelbert LM, Nagpal S: Transcriptional profiling of keratinocytes reveals a vitamin D-regulated epidermal differentiation network. J Invest Dermatol 2005, 124:778–785
34. Magerl M, Tobin DJ, Muller-Rover S, Hagen E, Lindner G, McKay IA, Paus R: Patterns of proliferation and apoptosis during murine hair follicle morphogenesis. J Invest Dermatol 2001, 116:947–955
35. Paus R, Stenn KS, Link RE: Telogen skin contains an inhibitor of hair growth. Br J Dermatol 1990, 122:777–784
36. Cascallana JL, Bravo A, Donet E, Leis H, Lara MF, Paramio JM, Jorcano JL, Perez P: Ectoderm-targeted overexpression of the glucocorticoid receptor induces hypohidrotic ectodermal dysplasia. Endocrinology 2005, 146:2629–2638
37. Cascallana JL, Bravo A, Page A, Budunova I, Slaga TJ, Jorcano JL, Perez P: Disruption of eyelid and cornea development by targeted overexpression of the glucocorticoid receptor. Int J Dev Biol 2003, 47:59–64
38. Pérez P, Page A, Bravo A, Del Rio M, Gimenez-Conti I, Budunova I, Slaga TJ, Jorcano JL: Altered skin development and impaired proliferative and inflammatory responses in transgenic mice overexpressing the glucocorticoid receptor. FASEB J 2001, 15:2030–2032
39. Priolo M, Lagana C: Ectodermal dysplasias: a new clinical-genetic classification. J Med Genet 2001, 38:579–585
40. Kellendonk C, Tronche F, Reichardt HM, Schutz G: Mutagenesis of the glucocorticoid receptor in mice. J Steroid Biochem Mol Biol 1999, 69:253–259
41. Li M, Chiba H, Warot X, Messaddeq N, Gerard C, Chambon P, Metzger D: RXR-alpha ablation in skin keratinocytes results in alopecia and epidermal alterations. Development 2001, 128:675–688
42. Li YC, Pirro AE, Amling M, Delling G, Baron R, Bronson R, Demay MB: Targeted ablation of the vitamin D receptor: an animal model of vitamin D-dependent rickets type II with alopecia. Proc Natl Acad Sci USA 1997, 94:9831–9835
43. Xie Z, Komuves L, Yu QC, Elalieh H, Ng DC, Leary C, Chang S, Crumrine D, Yoshizawa T, Kato S, Bikle DD: Lack of the vitamin D receptor is associated with reduced epidermal differentiation and hair follicle growth. J Invest Dermatol 2002, 118:11–16
44. Sharov AA, Weiner L, Sharova TY, Siebenhaar F, Atoyan R, Reginato AM, McNamara CA, Funa K, Gilchrest BA, Brissette JL, Botchkarev VA: Noggin overexpression inhibits eyelid opening by altering epidermal apoptosis and differentiation. EMBO J 2003, 22:2992–3003
45. Xia Y, Kao WW: The signaling pathways in tissue morphogenesis: a lesson from mice with eye-open at birth phenotype. Biochem Pharmacol 2004, 68:997–1001
46. Berger S, Bleich M, Schmid W, Cole TJ, Peters J, Watanabe H, Kriz W, Warth R, Greger R, Schutz G: Mineralocorticoid receptor knockout mice: pathophysiology of Na^+ metabolism. Proc Natl Acad Sci USA 1998, 95:9424–9429
47. Sundberg JP, Peters EM, Paus R: Analysis of hair follicles in mutant laboratory mice. J Investig Dermatol Symp Proc 2005, 10:264–270
48. Lopez GN, Webb P, Shinsako JH, Baxter JD, Greene GL, Kushner PJ: Titration by estrogen receptor activation function-2 of targets that are downstream from coactivators. Mol Endocrinol 1999, 13:897–909
49. Aszterbaum M, Feingold KR, Menon GK, Williams ML: Glucocorticoids accelerate fetal maturation of the epidermal permeability barrier in the rat. J Clin Invest 1993, 91:2703–2708
50. Kömüves LG, Hanley K, Jiang Y, Elias PM, Williams ML, Feingold KR: Ligands and activators of nuclear hormone receptors regulate epidermal differentiation during fetal rat skin development. J Invest Dermatol 1998, 111:429–433
51. Hanley K, Rassner U, Elias PM, Williams ML, Feingold KR: Epidermal barrier ontogenesis: maturation in serum-free media and acceleration by glucocorticoids and thyroid hormone but not selected growth factors. J Invest Dermatol 1996, 106:404–411
52. Ito N, Ito T, Kromminga A, Bettermann A, Takigawa M, Kees F, Straub RH, Paus R: Human hair follicles display a functional equivalent of the hypothalamic-pituitary-adrenal axis and synthesize cortisol. FASEB J 2005, 19:1332–1334
53. Slominski A, Wortsman J: Neuroendocrinology of the skin. Endocr Rev 2000, 21:457–487
54. Slominski A, Wortsman J, Kohn L, Ain KB, Venkataraman GM, Pisarchik A, Chung JH, Giuliani C, Thornton M, Slugocki G, Tobin DJ: Expression of hypothalamic-pituitary-thyroid axis related genes in the human skin. J Invest Dermatol 2002, 119:1449–1455
55. Slominski A, Wortsman J, Luger T, Paus R, Solomon S: Corticotropin releasing hormone and proopiomelanocortin involvement in the cutaneous response to stress. Physiol Rev 2000, 80:979–1020
56. Slominski A, Gomez-Sanchez CE, Foecking MF, Wortsman J: Metab-

olism of progesterone to DOC, corticosterone and 18OHDOC in cultured human melanoma cells. FEBS Lett 1999, 455:364–366
57. Slominski A, Gomez-Sanchez CE, Foecking MF, Wortsman J: Active steroidogenesis in the normal rat skin. Biochim Biophys Acta 2000, 1474:1–4
58. Slominski A, Wortsman J, Foecking MF, Shackleton C, Gomez-Sanchez C, Szczesniewski A: Gas chromatography/mass spectrometry characterization of corticosteroid metabolism in human immortalized keratinocytes. J Invest Dermatol 2002, 118:310–315
59. Slominski A, Zbytek B, Semak I, Sweatman T, Wortsman J: CRH stimulates POMC activity and corticosterone production in dermal fibroblasts. J Neuroimmunol 2005, 162:97–102
60. Slominski A, Zbytek B, Szczesniewski A, Semak I, Kaminski J, Sweatman T, Wortsman J: CRH stimulation of corticosteroids production in melanocytes is mediated by ACTH. Am J Physiol Endocrinol Metab 2005, 288:E701–E706
61. Deppe CE, Heering PJ, Viengchareun S, Grabensee B, Farman N, Lombes M: Cyclosporine a and FK506 inhibit transcriptional activity of the human mineralocorticoid receptor: a cell-based model to investigate partial aldosterone resistance in kidney transplantation. Endocrinology 2002, 143:1932–1941
62. Yamamoto S, Kato R: Hair growth-stimulating effects of cyclosporin A and FK506, potent immunosuppressants. J Dermatol Sci 1994, 7(Suppl):S47–S54
63. Gafter-Gvili A, Sredni B, Gal R, Gafter U, Kalechman Y: Cyclosporin A-induced hair growth in mice is associated with inhibition of calcineurin-dependent activation of NFAT in follicular keratinocytes. Am J Physiol Cell Physiol 2003, 284:C1593–C1603